The final publication is available at

http://doi.org/ 10.1039/c6cy00395h

Additional Information

Journal Name

ARTICLE

Effect of the C_α substitution on the ketonic decarboxylation of carboxylic acids over *m*-ZrO₂: the role of entropy

B. Oliver-Tomas,[a] F. Gonell,[a,b] A. Pulido,[a,†] M. Renz[a] and M. Boronat[a]

The kinetics of the ketonic decarboxylation of linear and branched carboxylic acids over *m*-ZrO₂ as catalyst has been investigated. The same apparent activation energy is experimentally determined for the ketonic decarboxylation of both linear pentanoic and branched 2-methyl butanoic acids, while the change in entropy for the rate determining step differs by nearly 50 kJ mol^{-1}. These results show that the difference in reactivity between linear and branched acids is due to entropic effects, and is related to the probability of finding the reactant molecules adsorbed and activated in a proper way on the catalyst surface.

1. Introduction

The ketonic decarboxylation has been widely applied for the industrial production of ketones from the corresponding acids.[1-3] This reaction converts two carboxylic acid molecules into a ketone molecule while releasing carbon dioxide and water:

$$R_1\text{-COOH} + R_2\text{-COOH} \rightarrow R_1\text{-CO-}R_2 + CO_2 + H_2O$$
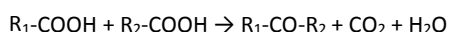
At present, the production of chemicals and fuels from biomass, instead of fossil fuels, is a topical research area in both academia and industry.[4-6] Biomass consists of a mixture of highly oxy-functionalized molecules whose carbon/oxygen ratio needs to be increased for production of fuels and chemicals, and one of the routes that combines the formation of a new C–C bond with deoxygenation is the aforementioned ketonic decarboxylation of carboxylic acids.[7,8] Hydrocarbon mixtures, with a particular interest in lubricants[8] and biofuels in the jet fuel range,[9-12] are obtained when starting from fatty acids and hexose derived pentanoic acid, respectively, by a synthesis sequence involving a ketonic decarboxylation step together with a hydrodeoxygenation step. A wide range of single and mixed metal oxides have been tested as catalysts for the ketonic decarboxylation reaction, and while an excellent performance and stability has been reported for transition metal oxides like TiO₂, Cr₂O₃, ZrO₂ or CeO₂, other metal oxides like MgO form metal carboxylates and are degraded under reaction conditions.[9,13-18] The different mechanistic theories proposed for the ketonic decarboxylation have been recently reviewed by

Resasco et al.[9] who conclude that, on high lattice energy oxides like TiO₂, Cr₂O₃, ZrO₂ or CeO₂, the reaction occurs on the catalyst surface and requires the presence of an α-hydrogen atom (H_α) in at least one of the reactant carboxylic acids.

Monoclinic zirconia is a highly active and selective catalyst for ketonic decarboxylation of a wide range of substrates, namely for linear carboxylic acids with two to eighteen carbon atoms.[19] The mechanism of ketonic decarboxylation of acetic acid was investigated by means of DFT calculations, and the kinetically favoured pathway involved formation of a β-keto acid intermediate by reaction of two non-equivalent fragments: a cationic acyl group resulting from dehydroxylation of the adsorbed acid, and an enolized carboxylate species formed through deprotonation of adsorbed acetate (Scheme 1).
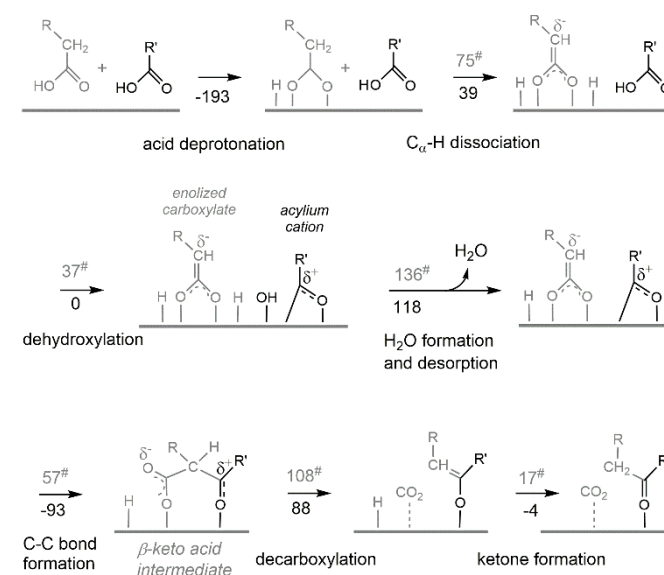
Scheme 1. Reaction mechanism for the ketonic decarboxylation of carboxylic acids over *m*-ZrO₂. DFT-D3 calculated reaction (black numbers) and activation (grey numbers with superscript #) energies for each step in the reaction between two acetic acid molecules (R= H, R'= CH₃) are shown. From ref. 19.

a. *Instituto Tecnología Química, Universidad Politécnica de Valencia–Consejo Superior de Investigaciones Científicas, Av. de los Naranjos, s/n, 46022 Valencia, Spain. boronat@itq.upv.es.*

b. *Departamento de Química Inorgánica y Orgánica, Universitat Jaume I, Av. Vicente Sos Baynat s/n, 12071 Castellón, Spain.*

† Current address: School of Chemistry, University of Southampton, Southampton, SO17 1BJ, United Kingdom.

This deprotonation step involves dissociation of a C_α–H bond (C_α is the carbon atom next to the carbonyl group), and therefore the conclusion was reached that ketonic decarboxylation of carboxylic acids without H_α atoms such as pivalic acid or 2,2,5,5-tetramethyladipic acid cannot occur through this mechanism.

Moreover, there is experimental evidence that the reactivity of carboxylic acids towards ketonic decarboxylation decreases with increasing degree of branching at the C_α atom.[9,15, 20] When ketonic decarboxylation takes place between two different carboxylic acids (R ≠ R' in Scheme 1) having H_α atoms, then a mixture of three ketones, the two symmetrical ones (R-CH$_2$CO-CH$_2$-R and R'-CO-R') and the asymmetrical one (R-CH$_2$-CO-R'), should be obtained with a statistical 1:1:2 ratio. A similar reactivity leading to a statistical product distribution has been found for linear carboxylic acids but, in the case of branched molecules, a non-statistical product distribution arising from a higher reactivity of carboxylic acids with smaller degree of C_α branching has been reported[15,19-25]. This issue has been recently addressed by Ignatchenko et al.,[20] and it has been explained by the existence of different zones in the reactor in relation to concentration of reactants. Thus, it is proposed that the most reactive carboxylic acid selectively reacts with itself producing a symmetrical ketone at the top section of the catalyst bed. Then, due to the shortage of this acid in the bottom section of the catalyst bed, the less reactive one reacts with itself producing a different symmetrical ketone, and only a little amount of the asymmetrical ketone is formed. While this study clearly explains the product distribution obtained in the ketonic decarboxylation of two different carboxylic acids, no reason is given for the higher reactivity of linear versus branched carboxylic acids. In this contribution we investigate the kinetics of the ketonic decarboxylation of pentanoic and 2-methylbutanoic acids to the corresponding symmetrical ketones, 5-nonanone and 3,5-dimethyl-4-heptanone, and demonstrate that entropic effects are the reason for the lower intrinsic reactivity of branched carboxylic acids.

2. Experimental Section

2.1. General

Pentanoic, 2-methylbutanoic, and pivalic acids were purchased from standard chemical suppliers, such as Acros or Aldrich, and used as received. Monoclinic zirconium oxide (m-ZrO$_2$) was obtained as pellets from ChemPur, Germany, with a surface area of 104 m^2 g^{-1}.

2.2. Ketonic decarboxylation in a fixed-bed, continuous-flow reactor

The reaction set-up used for ketonic decarboxylation has been described before.[19] For each reaction an adequate amount of fresh m-ZrO$_2$ (pellets, 0.4 – 0.8 mm) was diluted with silicon carbide, placed in the reactor and heated to the reaction temperature. At ambient pressure pentanoic acid or 2-methylbutanoic acid was passed through the reactor with a given molar flow rate (F) using nitrogen as carrier gas. For each reaction the catalyst amount (W) was adjusted to obtain adequate $W \cdot F^{-1}$. The product mixture was condensed at the exit of the reactor and analysed offline by gas chromatography with dodecane as external standard. Carbon mass balance was ≥ 97% in all cases.

The reaction products obtained as organic liquids were analysed with an Agilent 7890A apparatus equipped with a HP-5 column (30 m x 0.320 mm x 0.25 μm), and the substances were identified with a GC-MS apparatus Agilent 6890N, equipped with the same column and a mass selective detector Agilent Technologies 5973 Network.

2.3. Catalyst calcination treatment

m-ZrO$_2$ was calcined for 6 hours from room temperature to a final temperature between 923 – 1123 K with a heating rate of 3 K min^{-1} under N$_2$ flow.

2.4. Catalyst characterization

XRD measurements were performed by means of a PANalytical Cubix'Pro diffractometer equipped with an X'Celerator detector and automatic divergence and reception slits using Cu-Kα radiation (0.154056 nm). The mean size of the ordered (crystalline) domains (d) was estimated using the Scherrer equation. The equation can be written as $d = \frac{0.9\,\lambda}{\beta\,cos\theta}$, where λ is the X-ray wavelength, β is the line broadening at half the maximum intensity (FWHM), after subtracting the instrumental line broadening, in radians, and θ is the Bragg angle. The characterization by TEM was carried out in a JEM-2100F (JEOL) field emission microscope, at an accelerating voltage of 200 kV.

3. Results and Discussion

To evaluate the influence of the substitution pattern in α-position of the carboxylic acid in the ketonic decarboxylation rate, two different C$_5$ carboxylic acids were reacted with monoclinic zirconium oxide (m-ZrO$_2$). The intrinsic reactivity of pentanoic (a linear C$_5$ carboxylic acid with two H_α) and 2-methylbutanoic (a branched C$_5$ carboxylic acid with one H_α) acids to the corresponding symmetrical ketones, 5-nonanone and 3,5-dimethyl-4-heptanone, respectively, was investigated in separate reactions over m-ZrO$_2$ in a fixed-bed continuous-flow reactor. Experiments were carried out at steady state conditions during 30 min. In agreement with previous reports,[15,19-25] pentanoic acid exhibited good to complete conversion in the reaction temperature range investigated, 623 – 698 K, whereas 2-methylbutanoic acid was only partly converted (~30%) at the highest reaction temperature (698 K, see Figure 1, left). The competitive reactivity of pentanoic and 2-methylbutanoic acid was also directly investigated by performing the ketonic decarboxylation of a 1:1 mixture of both acids over m-ZrO$_2$ in the same temperature range (see Figure 1, right), and similar tendencies were observed as for the single reactions. Conversion of pentanoic acid was almost 90% at 648 K and complete at higher temperatures, whereas 2-

methylbutanoic acid required temperatures of 673 − 698 K for reaching significant conversions (20% – 40%).
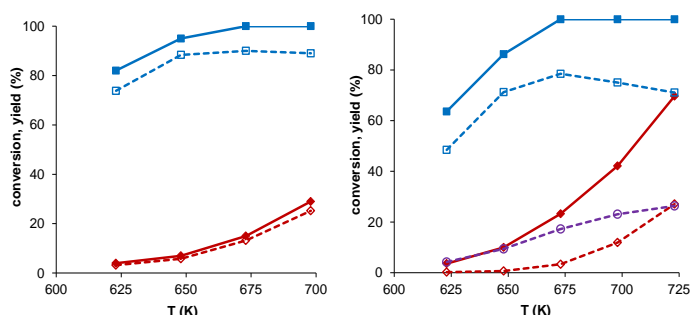

Figure 1. Ketonic decarboxylation of pure pentanoic and 2-methylbutanoic acids (left) and of a mixture of pentanoic and 2-methylbutanoic acids (right) over m-ZrO$_2$ at different reaction temperatures. Conversion of pentanoic (blue ■) and 2-methylbutanoic (red ♦) acids, and yield of the symmetrical 5-nonanone (blue □) and 3,5-dimethyl-4-heptanone (red ◊), and of the cross-ketonization product 3-methyl-4-octanone (purple ○) are plotted. Reaction conditions: W = 2,5 g catalyst, F = 8.5 g h^{-1} acid, nitrogen flow rate = 50 mL min^{-1}.

The yields of the corresponding symmetric and asymmetric ketones were also in agreement with the previously described results: 5-nonanone was the main product in the whole temperature range, while 3,5-dimethyl-4-heptanone and 3-methyl-4-octanone (the cross-ketonization product) were obtained in much lower yields, which increased when raising temperature.

In order to get quantitative information, initial reaction rates for the ketonic decarboxylation of pentanoic and 2-methyl-butanoic acids were measured in separate reactions at different temperatures (see Table 1 and Figure 2). As expected, the reaction rate for pentanoic acid decarboxylation is significantly higher (~30 times faster) than that obtained for 2-methyl-butanoic acid at all temperatures considered, confirming the lower reactivity of the branched carboxylic acid.
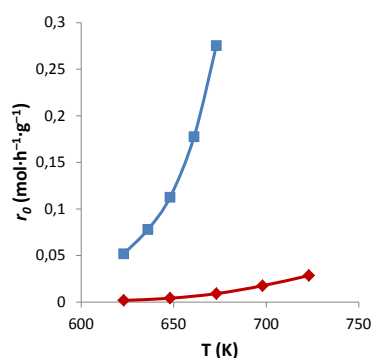

Figure 2. Initial reaction rates r_0 (in mol h^{-1} g^{-1}) for the ketonic decarboxylation of pentanoic (blue ■) and 2-methylbutanoic (red ♦) acids over m-ZrO$_2$ at different reaction temperatures. Reaction conditions: W = variable, mass flow rate = 36.0 g h^{-1}

(molar flow rate F = 0.353 mol h^{-1}) acid, nitrogen flow rate = 150 mL min^{-1}.

Table 1. Initial reaction rates r_0 (in mol h^{-1} g^{-1}) for the ketonic decarboxylation of pentanoic and 2-methylbutanoic (2MB) acids over m-ZrO$_2$ at different reaction temperatures.

|	r_0 (mol·h^{-1}·g^{-1})		
T (K)	pentanoic acid	2MB acid	$r_{pentanoic}/r_{2MB}$
623	5.172·10^{-2}	1.781·10^{-3}	29.0
636	7.788·10^{-2}		
648	1.125·10^{-1}	4.126·10^{-3}	27.3
661	1.776·10^{-1}		
673	2.753·10^{-1}	9.092·10^{-3}	30.3
698		1.756·10^{-2}	
723		2.845·10^{-2}	

Under the reaction conditions chosen, the catalyst surface is saturated with substrate molecules and the reaction rate is independent of the partial pressure of acid in the feed flow (see Figure S1 and detailed description in the ESI). Therefore, the initial reaction rate r_0 can be approximated to the kinetic constant k, that is, r$_0$ = k. According to transition state theory, the rate constant k is expressed as:

$$k = \frac{k_B\,T}{h}\,e^{\Delta S^{\ddagger}/R}\,e^{-\Delta H^{\ddagger}/RT}$$

or

$$Lnk = Ln\left(\frac{k_B\,T}{h}\right) + \frac{\Delta S^{\ddagger}}{R} - \frac{\Delta H^{\ddagger}}{R}\left(\frac{1}{T}\right)$$

where k_B is the Boltzmann constant, h is Planck's constant and R is the ideal gas constant. Activation energies $\Delta H^{\ddagger}$, were obtained from the slope of the plots of the logarithm of initial reaction rate Lnk versus the inverse of temperature $1/T$, as shown in Figure 3. Unexpectedly, the calculated activation energies obtained for pentanoic acid and 2-methyl-butanoic acid decarboxylation are almost equivalent, 116.1 and 105.1 kJ mol^{-1}, respectively. However, the change in entropy for the transition state $\Delta S^{\ddagger}$ values obtained from the intersection with the ordinate of the same plots in Figure 3 are clearly different, –90 and –135 J mol^{-1} K^{-1} for pentanoic and 2-methyl-butanoic acids, respectively.
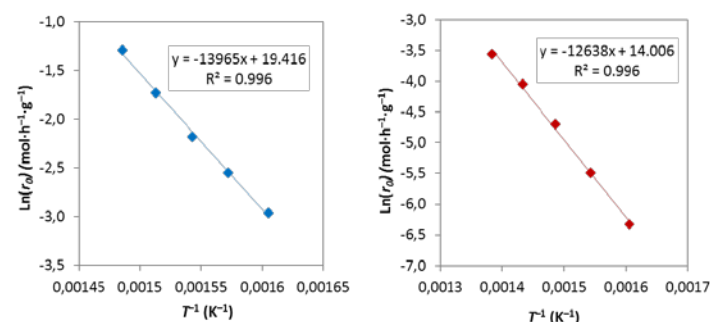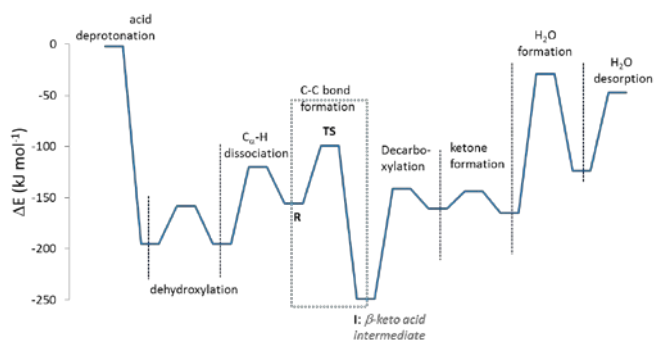
Figure 3. Plot of ln(r) against T^{-1} for pentanoic (blue ■) and 2-methylbutanoic (red ♦) acids. The regression parameters of the linear fitting of data are also shown.

These values indicate that the difference in reactivity between linear and branched acids has to be attributed to entropic effects, and can be related to the probability of finding the reactant molecules adsorbed and activated in a proper way.

To better understand these observations we revised our previous theoretical study of acetic acid decarboxylation over m-ZrO$_2$,[19] which showed that the reaction mechanism involves formation of a dianionic enediolate by removal of an H$_\alpha$ from adsorbed acetate (C$_\alpha$–H dissociation step in Scheme 1) and an acylium cation by dehydroxylation of a second acetic acid molecule. At some point in the reaction pathway, water is formed and desorbs from the surface. Then, a nucleophilic attack of the dianionic enediolate onto the acylium cation leads to formation of the β-keto acid intermediate (C–C bond forming step in Scheme 1) which, after breaking another C–C bond that yields CO$_2$ (decarboxylation step) ends in the ketone enolate that is finally protonated to produce the desired ketone (ketone formation step). The activation and reaction energies previously calculated for acetic acid decarboxylation are included in Scheme 1, and the global energy profile is depicted in Figure 4. Adsorption and deprotonation of acetic acid was found highly exothermic (–195 kJ mol^{-1}) and barrier less, in agreement with the experimental observation that under reaction conditions the catalyst surface is completely covered by deprotonated carboxylic acid. The intrinsic activation energy for dehydroxylation (37 kJ mol^{-1}) was lower than that for dissociation of C$_\alpha$–H bond (75 kJ mol^{-1}), this last step being also thermodynamically unfavourable. As recently discussed by Ignatchenko et al., dissociation of the C$_\alpha$–H bond is a reversible process significantly shifted toward the initial carboxylate under reaction conditions.[20] As regards the influence of branching on this first part of the mechanism, Ignatchenko investigated by means of DFT calculations the adsorption and deprotonation of acetic, propanoic and isobutyric acids over m-ZrO$_2$, as well as the dissociation of a C$_\alpha$–H bond in the resulting carboxylates. He found these elementary steps quite insensitive to the degree of C$_\alpha$ substitution, with all calculated adsorption and activation barriers ranging within 2 kJ mol^{-1}.[21,22] It is to be noted here that these DFT energies are only electronic, that is, they do not include entropy changes. A similar result has been now obtained for the dehydroxylation step (see Figure S2 and detailed description in the ESI).

Figure 4. Calculated energy profile at the DFT-D3 level for ketonic decarboxylation of acetic acid over m-ZrO$_2$. Data from Ref. 19.

Dehydroxylation of pivalic acid, taken as the most sterically hindered C$_5$ acid, over m-ZrO$_2$ occurs through a transition state similar to that previously described for acetic acid, with a calculated intrinsic activation energy of 33 kJ mol^{-1} and, what is more important, with no apparent steric hindrance due to the three substituting methyl groups.

After C$_\alpha$–H dissociation and dehydroxylation, the C–C bond forming step produces the β–ketoacid intermediate, and its subsequent decarboxylation yields CO$_2$ and the surface ketone precursor. The intrinsic activation energy for the C–C bond forming step in the case of acetic acid yielding the β–keto acid intermediate (57 kJ mol^{-1}) was found lower than that of decarboxylation (108 kJ mol^{-1}), but it is clear that the ΔS entropy term will favour the decarboxylation reaction that involves bond dissociation, and will destabilize the transition state for the C–C bond forming step that involves coupling of fragments and formation of new bonds. Assuming a similar reaction mechanism for linear and branched acids, it is to be expected that the less favourable entropy change experimentally determined for the branched 2-methylbutanoic acid as compared to linear pentanoic acid should be related to the C–C bond forming step. As clearly exposed by Ignatchenko et al.,[20] it is necessary for this coupling step to occur that the enolized carboxylate and the acylium cation fragments are co-adsorbed in close proximity and with the correct orientation, so that the reaction rate will depend on the concentration of fragments adequately distributed on the catalyst surface.

The optimized geometries of the reactant R, transition state TS and β–keto acid intermediate I involved in the C–C bond forming step of the acetic acid ketonic decarboxylation are depicted in Figure 5, together with a schematic representation of an equivalent transition state TS1' for more substituted acids.
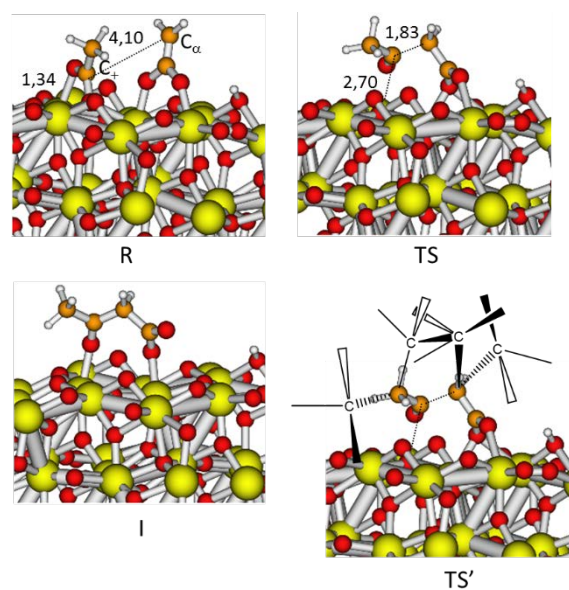

Figure 5. PW91 optimized geometries of reactant (R), transition state (TS) and β–keto acid intermediate (I) involved in the C–C bond forming step of acetic acid decarboxylation, and

schematic representation of a similar transition state TS' with bulkier alkyl groups. Zr, O, C and H atoms are depicted as yellow, red, orange and white balls, respectively. Adapted from Ref. 19. It can be observed that the presence of bulky alkyl groups in the organic fragments decreases the degrees of freedom of the system with the concomitant loss in entropy. Thus, for instance, rotation of the methyl group in dehydroxylated acetic acid is free, but it is hindered in dehydroxylated propanoic or 2-methylpropanoic acids due to steric impediments. On the other hand, while the three substituents in the C_α of the dehydroxylated fragment of acetic acid are equivalent, they are not in the case of more substituted acids. As an example, only one out of three possible orientations of these substituents in 2-methylpropanoic reactant structure R allows an adequate orientation of the two fragments and the formation of the new C–C bond. This provides a possible explanation for the experimentally determined role of entropy in the lower reactivity of branched carboxylic acids.

Taking a deeper look at the optimized geometry of the transition state for the C-C bond forming step in Figure 5, it appears that the steric repulsion between the alkyl groups in the case of branched carboxylic acids could be minimized if both fragments were not placed at the same level on a perfect surface, but at some type of edge defect. The possibility of a structure-reactivity relationship was considered at this point, and four m-ZrO$_2$ catalyst samples with different crystallite size were prepared by calcining the same initial sample at increasing temperatures. Selected TEM micrographs of the four samples are shown in Figure 6, and BET area and particle size data are summarized in Table 2. The number of surface Zr sites in each sample was estimated assuming a surface density of 1.0144×10^{19} Zr atoms per m^2, that is, 1.6842×10^{-5} moles of Zr atoms per m^2, which was obtained from the periodic slab model of the extended ($\bar{1}$11) surface used in the DFT study.
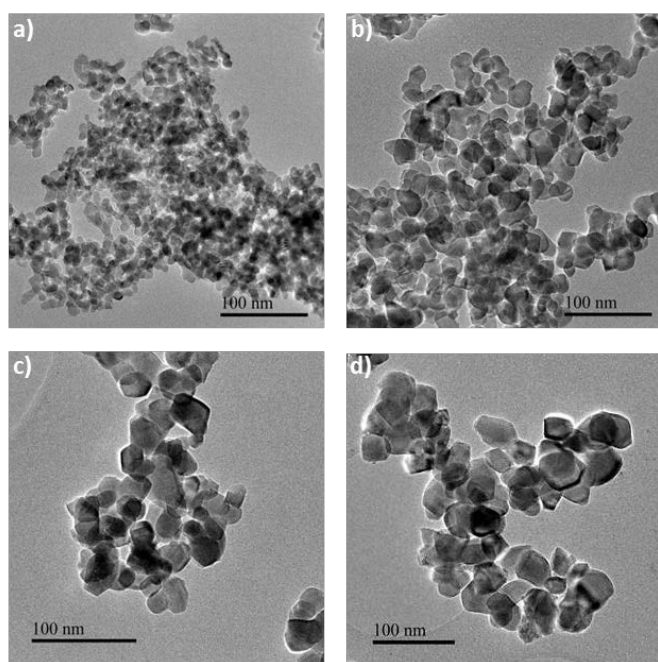

Figure 6. TEM micrographs of ZrO$_2$ samples a) as purchased and calcined at b) 923 K, c) 1023 K and d) 1123 K.

Table 2. Characterization of m-ZrO$_2$ catalyst samples calcined at increasing temperature.

Catalyst Sample	Calcination T (K)	Crystal size (nm)	BET area (m^2 g^{-1})	Surface Zr sites x 10^4 (mol g^{-1})
1	Non calcined	9.5	104.0	17.516
2	923	14.4	53.4	8.994
3	1023	20.1	35.4	5.962
4	1123	24.5	21.7	3.655

Table 3. Initial reaction rates r_0 (in mol h^{-1} g^{-1}) and turnover frequencies TOF (in h^{-1}) for the ketonic decarboxylation of pentanoic and 2-methylbutanoic (2MB) acids over m-ZrO$_2$ samples with different particle size and surface area.

Catalyst Sample	r_0 pent (mol·h^{-1}·g^{-1})	r_0 2MB (mol·h^{-1}·g^{-1})	TOF$_{pent}$ (h^{-1})	TOF$_{2MB}$ (h^{-1})	TOF$_{pent}$/ TOF$_{2MB}$
1	0.27525	0.00909	157.1	5.20	30.3
2	0.12590	0.00356	140.0	3.96	35.4
3	0.08997	0.00183	150.9	3.07	49.2
4	0.04617	0.00096	126.3	2.62	48.2

The ketonic decarboxylation of pentanoic acid and 2-methyl-butanoic acids was studied in separate reactions over these four m-ZrO$_2$ samples, and turnover frequencies (TOF) were calculated by dividing the measured reaction rates by the number of surface Zr sites (see Table 3). Again, the reactivity of the linear pentanoic acid is considerably higher than that of the branched acid on all samples. Interestingly, the difference in reactivity measured by the ratio TOF$_{pent}$/TOF$_{2MB}$ clearly increases when particles become larger. Since as particle size increases a higher ratio of Zr atoms in planes with respect to edges and corners exists, the results obtained would support the hypothesis that the ketonic decarboxylation of 2-methyl-butanoic acid preferentially occurs on Zr atoms located at corners and edges of the crystallites, where the steric repulsion between the alkyl groups in the branched compounds will have a lower impact in the conformation of the transition state for the C-C bond forming step.

Conclusions

In summary, the kinetic study of the ketonic decarboxylation of linear and branched carboxylic acids over m-ZrO$_2$ catalyst confirms the lower reactivity of carboxylic acids with a higher degree of substitution in α-position. The novelty of this study is the similar activation energies experimentally determined for linear and branched carboxylic acids, and the conclusion that the difference in reactivity is only due to entropic effects. The probability of finding the enolized carboxylate and the acylium cation fragments co-adsorbed in close proximity and with the

correct orientation on the catalyst surface determines the overall reaction rate of the process.

Acknowledgements

Notes and references

‡ Footnotes relating to the main text should appear here.

1   C. Friedel, C. *Justus Liebigs Ann. Chem.* 1858, **108**, 122–125.
2   W. L. Howard in *Encyclopedia of Chemical Technology (Kirk-Othmer)*, 4th ed., Wiley-Interscience, New York, **1998**, vol. 1, pp. 176–194.
3   Siegel, H.; Eggersdorfer, M. *Ullmann's Encyclopedia of Industrial Chemistry*; VCH Weinheim, **1990.**
4   G. W. Huber, S. Iborra and A. Corma, *Chem. Rev.* **2006**, *106*, 4044–4098.
5   A. Corma, S. Iborra and A. Velty, *Chem. Rev.* **2007**, *107*, 2411–2502.
6   J. N. Chheda, G. W. Huber and J. A. Dumesic, *Angew. Chem. Int. Ed.* **2007**, *47*, 7164–7183.
7   M. Renz, *Eur. J. Org. Chem.* **2005**, 979–988.
8   A. Corma, M. Renz and C. Schaverien, *ChemSusChem* **2008**, *1*, 739–741.
9   T. N. Pham, T. Sooknoi, S. P. Crossley and D. E. Resasco, *ACS Catal.* **2013**, *3*, 2456–2473.
10 J. C. Serrano-Ruiz, D. Wang and J. A. Dumesic, *Green Chem.* **2010**, *12*, 574–577.
11 D. Martin Alonso, J. Q. Bond and J. A. Dumesic, *Green Chem.* **2010**, *12*, 1493–1513.
12 A. Corma, B. Oliver-Tomas, M. Renz and I. L. Simakova, *J. Mol. Catal. A: Chem.* **2014**, *388,* 116–122.
13 S. Rajadurai, *Catal. Rev.–Sci. Eng.* **1994**, *36*, 385–403.
14 M. Glinski, J. Kijenski and A. Jakubowski, *Appl. Catal. A-Gen.* **1995**, *128*, 209–217.
15 R. Pestman, R. M. Koster, A. v. Duijne, J. A. Z. Pieterse and V. Ponec, *J. Catal.* **1997**, *168*, 265–272.
16 K. Parida and H. K. Mishra, *J. Mol. Catal. A-Chem.* **1999**, *139*, 73–80.
17 T. S. Hendren and K. M. Dooley, *Catal. Today* **2003**, *85*, 333–351.
18 R. Martinez, M. C. Huff and M. A. Barteau, *J. Catal.* **2004**, *222*, 404–409.
19 A. Pulido, B. Oliver-Tomas, M. Renz, M. Boronat and A. Corma, *ChemSusChem* **2013,** *6*, 141–151.
20 A. V. Ignatchenko, J. S. DeRaddo, V. J. Marino and A. Mercado, *Appl. Catal. A: General* **2015**, *498*, 10–24.
21 A. V. Ignatchenko and E. Kozliak, *ACS Catalysis* **2012**, 1555–1562.
22 A. V. Ignatchenko, *J. Phys. Chem. C* **2011**, *115*, 16012–16018.
23 M. A. Jackson and S. C. Cermak, *Appl. Catal. A: General* **2012**, *431-432*, 157–163.
24 N. D. Plint, N. J. Coville, D. Lack, G. L. Nattrass and T. Vallay, *J. Mol. Catal. A: Chem.* **2001**, *165*, 275–281.
25 S. D. Randery, J. S. Warren and K. M. Dooley, *Appl. Catal. A: General* **2002**, *226*, 265–280.